STAFF SUMMARY SHEET

	TO	ACTION	SIGNATURE (Surname), GRADE AND DATE		TO	ACTION	SIGNATURE (Surname), GRADE AND DATE
1	DFP	sig	WOHLWEND, Lt Col, 20Nov13	6			
2	DFER	approve	Kraus, Col 22Nov13	7			
3	DFP	action		8			
4				9			
5				10			

SURNAME OF ACTION OFFICER AND GRADE	SYMBOL	PHONE	TYPIST'S INITIALS	SUSPENSE DATE
Lane, Major	DFP	333-2460	GPA	20131130

SUBJECT		DATE
Clearance for Material for Public Release	USAFA-DF-PA- 542	20131120

SUMMARY

1. PURPOSE. To provide security and policy review on the document at Tab 1 prior to release to the public.

2. BACKGROUND.
Authors: G. Andersen, P. Gelsinger-Austin, F. Ghebremichael, R. Gaddipati and P. Gaddipati

Title: Fast, compact, autonomous holographic adaptive optics

Document type: Journal Paper

Description: In this paper, the authors detail experiments conducted into a novel holographic adaptive optics system.

Release Information: This document is being submitted for publication in Optics Express

Previous Clearance information: None

Recommended Distribution Statement:
Distribution A, Approved for public release, distribution unlimited.

3. DISCUSSION. This research has been funded by AFOSR and JTO.

4. VIEWS OF OTHERS. N/A

5. RECOMMENDATION. Sign coord block above indicating document is suitable for public release. Suitability is based solely on the document being unclassified, not jeopardizing DoD interests, and accurately portraying official policy.

// signed //

CORY T. LANE, Maj, USAF
Director of Research
Department of Physics

Tabs
1. HALOS OE paper

Fast, compact, autonomous holographic adaptive optics

Geoff Andersen,[1,2*] Paul Gelsinger-Austin[2], Ravi Gaddipati[2], Phani Gaddipati[2] and Fassil Ghebremichael[2]

[1]*Laser and Optics Research Center, HQ USAFA/DFP, Ste 2A31, 2354 Fairchild Dr., US Air Force Academy, CO 80840 , USA*

[2]*HUA Inc., 1532 Shane Circle, Colorado Springs, CO 80907 USA*

*huainc@comcast.net

Abstract: We present a closed-loop adaptive optics system based on a holographic sensing method. The system uses a multiplexed holographic recording of the response functions of each actuator in a deformable mirror. By comparing the output intensity measured in a pair of each photodiodes, the absolute phase can be measured over each actuator location. From this a feedback correction signal applied to the input beam without need for a computer. The sensing and correction is applied to each actuator in parallel, so the bandwidth is independent of actuator number. We demonstrate a working system using a 32-actuator MEMS deformable mirror operating at over 100kHz and without a computer in the loop.

OCIS codes: (110.1080) Active or adaptive optics; (090.0090) Holography; (010.1285) Atmospheric correction; (090.1000) Aberration compensation.

References and links

1. J. M. Geary, *Introduction to wavefront sensors*, SPIE Press, (1995).
2. R. Dyson, *Principles of adaptive optics* 2nd Ed., Academic Press (1998).
3. F. Roddier, *Adaptive optics in astronomy*, Cambridge Press (1999).
4. M. A. A. Neil, J. Booth and T. Wilson, "New modal wave-front sensor: a theoretical analysis," Opt. Soc. Am. A **17**, 1098-1107 (2000).
5. M. A. A. Neil, J. Booth and T. Wilson, "Close-loop aberration correction by use of a modal Zernike wave-front sensor," Opt. Lett. **25**, 1083-1085 (2000).
6. F. Ghebremichael, G. P. Andersen and K. Gurley, "Holography-based wavefront sensing," Appl. Opt. **47**, A62-A69 (2007).
7. A. D. Corbett et al. "Designing a holographic modal wavefront sensor for the detection of static ocular aberrations," J. Opt. Soc. Am. A **24**, 1266-1275 (2007).
8. G. P. Andersen et al. "Holographic wavefront sensor," Opt. Eng. **48**, 085801 (2009).
9. S. K. Mishra et al. "Differential modal Zernike wavefront sensor employing a computer-generated hologram: a proposal," Appl. Opt. **48**, 6458-6465 (2009).
10. L. Changhai et al "Modal wavefront sensor based on binary phase-only multiplexed computer-generated hologram," Appl. Opt. **49**, 5117-5124 (2010).
11. A. Zepp, "Holographic wavefront sensing with spatial light modulator in context of horizontal light propagation," Proc. SPIE **8535**, 85350I-1-10 (2012).
12. S. Dong, T. Haist, and W. Osten, "Hybrid wavefront sensor for the fast detection of wavefront disturbances," Appl. Opt. **51**, 6268-6274 (2012).

1. Introduction

Traditional adaptive optics systems use wavefront sensors that require a significant amount of computational overhead [1-3]. This includes the measurements as well as the derivation of phase information from those measurements. Additionally, wavefront phase is

usually expressed using some orthogonal basis set such as Zernike polynomials which then has to be deconvolved in order to derive particular actuator motions for closed-loop correction. One approach by the author and others [4-12], involves the use of a multiplexed hologram constructed by recording the maximum and minimum expected phase amplitudes of any number of Zernike modes. While this method has been shown to work, it suffers from a significant loss of efficiency as additional pair of holograms are multiplexed in the same location. Additionally, there is still the large amount of computational overhead in translating the final Zernike polynomial information into actuator motion in the phase corrector.

Here we present an alternative solution which uses a multiplexed hologram specially constructed to directly analyze the wavefront error based on actuator response functions. Essentially this modifies the previous holographic adaptive optics approaches by recording "modes" that are based on the actual response functions of each actuator. In operation, the phase information is derived from fast photodetector measurements of stationary reconstructed focal spots. Both the detection, sensing and corrective feedback are achieved with minimal, parallel computations. The result is a simple, compact system which is orders of magnitudes faster than conventional systems while being easily scaled to millions of actuators without loss of speed.

2. Theory

To best understand the operation of the holographic adaptive optics system it is often instructive to consider the construction of the holographic optical element. For our system we used an optical recording scheme, though with a good knowledge of the response functions of the deformable mirror (DM) a computer generated hologram is an equally viable solution. In our scheme a plane wave is reflected off an actuator in the deformable mirror that has been pushed to its maximum extent to impose some local phase delay (Fig. 1a). A hologram is recorded between this object beam and a convergent reference beam focused to some distant point A. Note that the property of a hologram is such that if the initial recording geometry for the actuator and input object beam remained the same, such a hologram would reconstruct a beam focused to this same point A.

We now record a second hologram on the first – this time with the actuator pulled to its maximum extent to give the maximum phase delay, and a reference beam focused to a different point B (Fig. 1b). If the actuator is now set to some arbitrary value between maximum and minimum phase delay, the object beam created does not match either of the recording cases. As such, the imperfect phase matching results in the reconstruction of two focused beams (Fig. 1c). The phase mismatch also imposes a curvature term onto each beam that gives rise to a slight focus to one and defocus to the other. By measuring the power transmitted through pinholes located at points A and B it is possible to derive a simple, direct relationship between focal spot intensity ratio and phase.

The procedure above describes the method for detecting phase over a given actuator location. To create a general wavefront sensor, a separate pair of multiplexed holograms are recorded for each actuator in the same manner. If we now take an input beam that fills the entire aperture and reflect this off the deformable mirror and on to the hologram, many pairs of focused beams are reconstructed (Fig. 1d). Note that the actual spatial arrangement of the focal spots or actuators is not critical but will most likely be determined by the geometry of the detector used.

In essence, where a Shack-Hartmann sensor detects local tilt over a given subaperture, the holographic wavefront sensor is measuring curvature. A key difference, however, is that with global tip/tilt removed, the focal spots remain centered on the pinholes and detectors. The phase is found simply by measuring an error function based on the relative power through each pinhole - something which can be accomplished at bandwidth of 100kHz rates or higher (assuming sufficient light flux) even using inexpensive photodetectors.

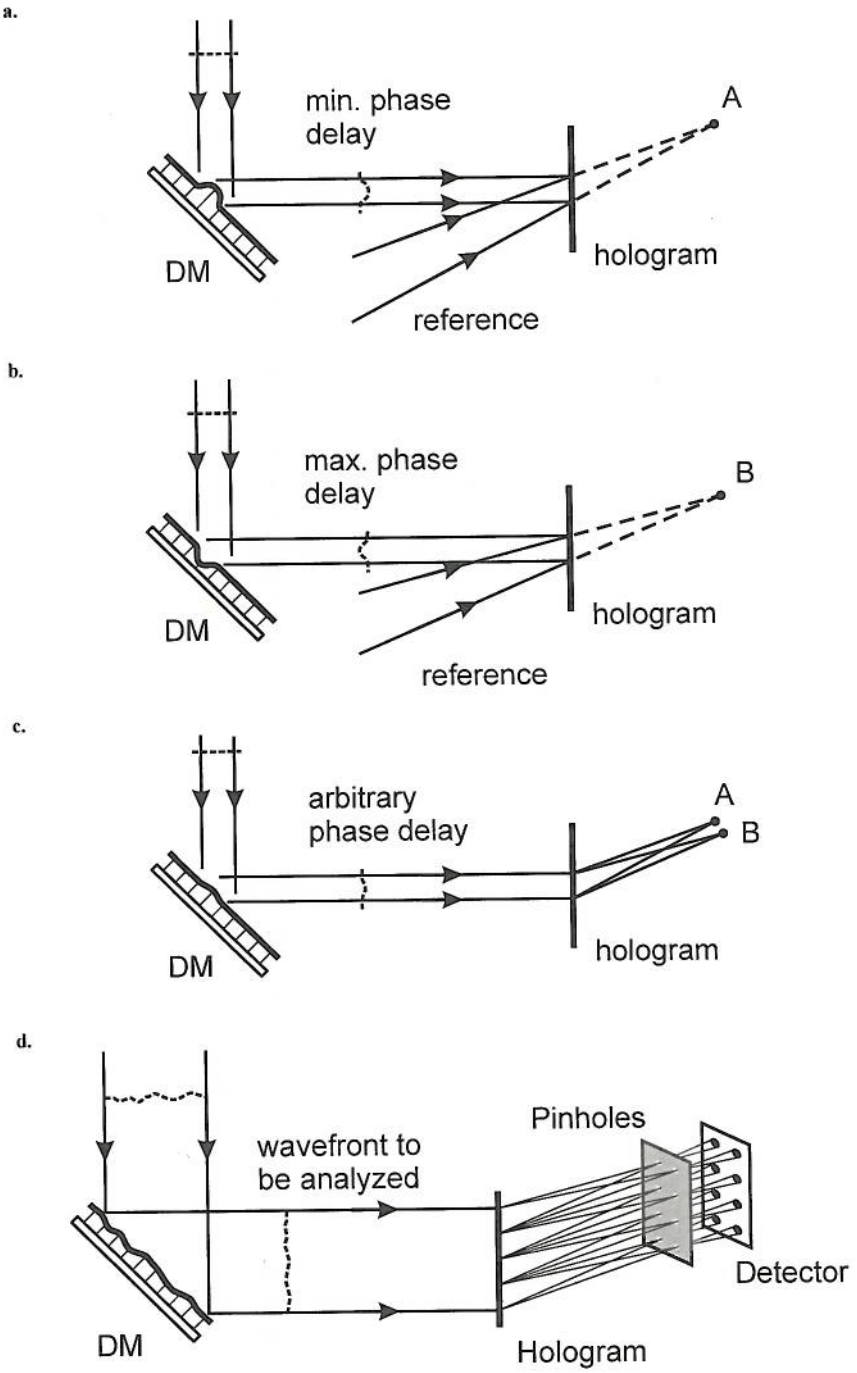

Fig. 1. a. The first recording is made with the actuator pushed to its maximal extent. **b.** A second hologram is recorded on the first with the actuator fully pulled and a reference beam focused to B. **c.** An input beam with arbitrary phase will reconstruct two focused beams to points A & B. d. A filled wavefront generates one pair of foci for each actuator.

In conventional holography we can define the recorded hologram by the interference pattern formed between an object beam, $O(x,y)=oe^{-i\phi}$ and plane wave reference beam $R(x,y)=re^{ikxsin\theta}$:

$$I(x,y) = [R+O][R+O]^* = r^2 + o^2 + 2ro\cos[kx\sin\theta + \emptyset] \quad (1)$$

In general operation, the beam reflected from an actuator will have the same form as the original object beam, but with some additional curvature term $C(x,y)O(x,y)$. In such a case this input beam will reconstruct a number of beams:

$$W(x,y) = I(x,y)C(x,y)O(x,y) = COR^2 + COO^2 + CO^2R^* + CORO^* \quad (2)$$

Here we see that he first term in this expression is simply the original object wave modified by the curvature term – giving rise to an accompanying change in the focal length of the reconstructed beam.

Fig. 2a shows a schematic of the reconstruction geometry for a portion of the beam reflected from a single actuator. With a pair of multiplexed holograms, this single beam will diffract from the hologram to reconstruct two focused beams to two fixed pinholes. In the figure we see the effect of the actuator driven to the two extremes (maximum push and pull) as indicated by the solid and dashed lines respectively. Note that for the desired flat condition, the light transmitted through the pinholes will be equalized, as neither beam will be perfectly in focus.

In order to model the transmitted power, we define a recording reference beam with radius of curvature R and wave number k,

$$E_{ref} = E_{0,ref}e^{-ik/2R} \quad (3)$$

and disturbance beam E_{err} with an error phase, $W(r)$, where

$$W(r) = \epsilon e^{-r^2/2\sigma^2} \quad (4)$$

with error magnitude ϵ, and the radial extent of the influence function of the actuator, s, adequately modeled as a Gaussian. Paraxial beam propagation through the sub-aperture illumination diameter of $2a$ results in the electric field function for the focused beam in the far-field as:

$$E(r) = E_0 e^{i\varphi(r)} \quad (5)$$

with aperture function ξ,

$$\varphi(r) = \frac{ik}{2R} + \epsilon W(r)\,\xi(r-a) \quad (6)$$

Rather than using a simple ratio of powers in the sensor pairs, we use a fractional energy difference as the error function, where $E = (Va-Vb)/(Va+Vb)$. This function has the advantage that it is invariant under changing input power and largely insensitive to stray background illumination. For an ideal actuator varied from fully pulled to pushed positions, the resultant error function is shown in Fig. 2b. With the MEMS mirror used in our experiments detailed here, the actuator motion is nonlinear with applied voltage, having an approximately quadratic response. As such, if we plot the modeled error function against voltage we get the asymmetric curve as shown in Fig. 2c.

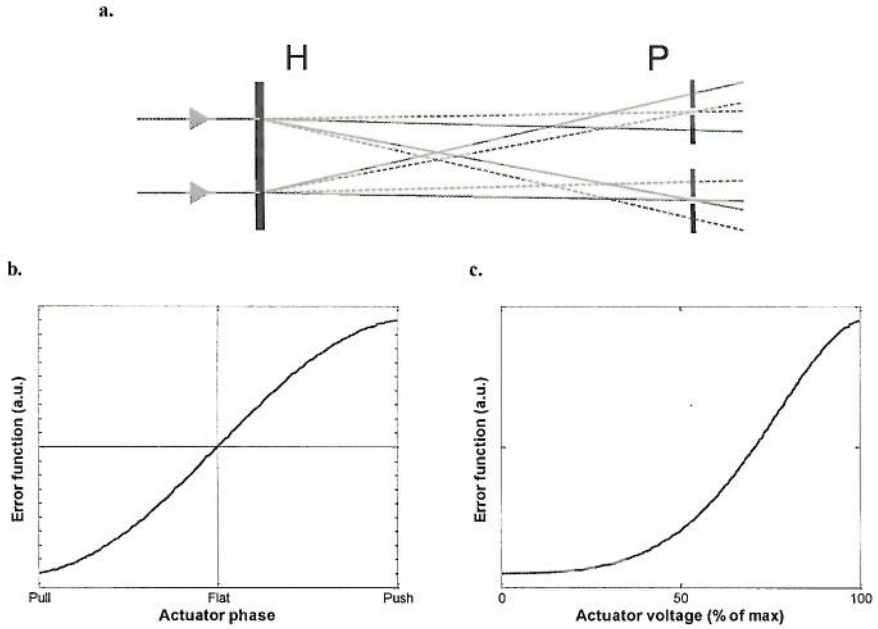

Fig. 2. a. A schematic of the reconstruction for a beam reflected off a single actuator, diffracting from the hologram (H) to produce two beams focused on two pinholes (P). The two reconstruction conditions are shown as the actuator is varied from maximum push to pull. A model of the HALOS error function is shown plotted against actuator position (**b.**) and actuator voltage (**c.**).

The key here is that the error function is always singly determined for a particular actuator voltage. Using this information the actuators can then be manipulated under one-to-one feedback control to correct for any wavefront errors. This avoids the high computational overhead associated with conventional adaptive optics schemes that require deconvolving wavefront phase from one global basis set to another, so a simple circuit can manage full closed-loop correction up to MHz rates. Furthermore, since the actuators are controlled in parallel, the system bandwidth is the same for one actuator as it is for thousands or more.

3. Experiment

We constructed a prototype holographic adaptive laser optics system (HALOS) using a 32-element Boston Micromachines micro-electromechanical deformable mirror (MEMS-DM). This mirror operates by deforming a continuous facesheet by electrostatic attraction and the nominal flat condition is achieved by setting the voltage on all actuators to 50% of their maximum. The "push" condition is achieved by reducing the applied voltage to an actuator and allowing the mirror to relax. We achieved 0.36μm stroke of pull and 0.33μm of push using a custom-made driver. Note that the holographic adaptive optics concept cannot be made to work with a segmented mirror as it is insensitive to discontinuities which can lead to a 2π modulus phase shift ambiguity.

We recorded 64 holograms (32 multiplexed pairs) using a cw Nd:YAG laser (λ = 532nm). Approximate layouts of the recording and reconstruction layouts are shown in Fig. 3. Motorized stages were used to move an aperture stop and reposition the fiber-fed reference beam to ensure overlap and correct pointing for each exposure. To eliminate diffractive effects, the aperture is imaged onto the DM which is, in turn, imaged onto the plane of the hologram. For larger deformable mirrors, with small distances between the DM and hologram, this may not be necessary.

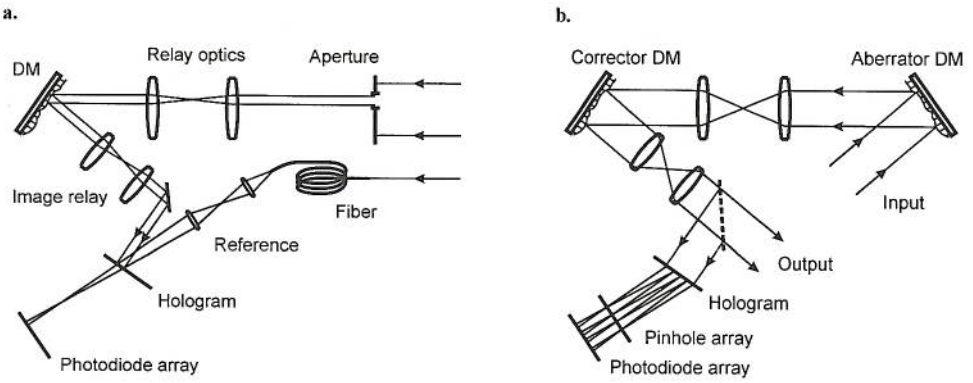

Fig. 3. a. Recording. An aperture isolates a particular actuator while the reference beam is formed from a coherent beam directed through a fiber and focusing optics. **b.** Replay. The aperture is replaced by a deformable mirror for testing. Light not directed onto the sensor forms the corrected output.

The diameter of the illumination patch for each actuator is approximately 0.5mm. In designing the holographic wavefront sensor it is important to choose an optimum illumination patch isolating the actuator of interest. Too large, and the hologram is unnecessarily recording a redundant extent of flat mirror which will reduce efficiency. Too small, and the hologram will not be recording the full extent of the actuator deformation relative to some global "flat" condition. Our modeling (verified by trial and error) shows that an ideal patch size is 1.2-1.6 times the interactuator spacing which is 0.3mm for our DM.

Phase transmission holograms were recorded on dichromated gelatin plate film with 20mW per beam and 50ms exposure per hologram. The angle between input beams was approximately 20 degrees on average. Optimizing efficiency was not a primary concern, but we easily managed a total input to output beam diffraction efficiency of 5% - or approximately 100pW per beam for the minimum usable input beam power of 130nW. Here we also note that the system can be adapted to work equally well with transmission, reflection or surface relief holograms, intensity or phase or in any type of medium. We have also demonstrated the possibility of using holograms recorded at one wavelength for reconstruction at another, thus making it possible for HALOS to operate in the infrared. In such a case, however, allowances have to be made for changes in geometry resulting from dispersion by the grating.

Reconstruction was achieved with a diffraction limited, collimated beam illuminating the entire DM aperture, producing 64 focused spots. We fabricated an array of 350 micron pinholes to isolate each focused spot. The light transmitted through each pinhole was collected by 64 elements of a SensL 4p9 avalanche photodiode array. Pairs of these input voltages were then used to generate an error signal for a particular actuator, as defined earlier. By cycling any actuator through its entire range of motion we can measure the error function – an example of which is shown in Fig. 4a. This data compares well with our model as shown in Fig. 2c, with the slight difference being due to a minor asymmetry in the mirror shape for the push and pull conditions.

For an ideal system with no cross-talk, the motion of one actuator will not give rise to a measurable error signal in a neighboring channel. However, since we have a continuous facesheet deformable mirror, the influence function is such that there will always be some inter-actuator cross-talk. Thus, even driving a single actuator in isolation, a change in the error function will not only be measured for the correct channel, but for the neighboring (stationary) elements as well. We measured this cross-talk for one actuator as shown in Fig. 4b, where we

see that moving one actuator through its entire range results in a minimal change in the error function measured in the neighboring 8 actuators.

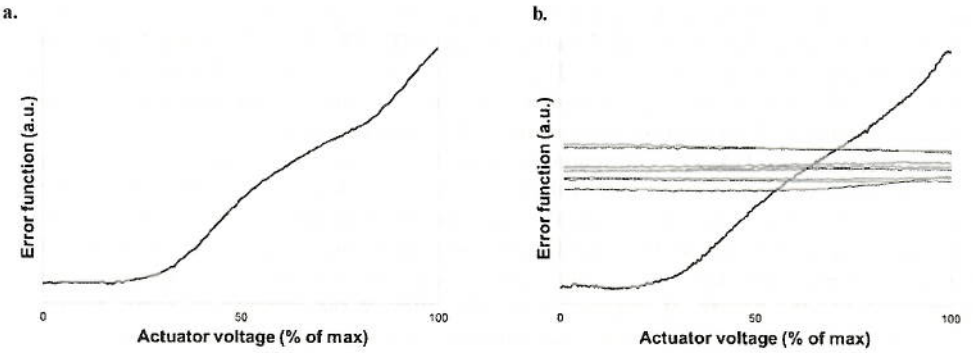

Fig. 4. a. The error function measured for a single actuator driven through the full range of motion. **b.** The error functions simultaneously recorded for the correct actuator channel, as well as the neighboring channels as the single actuator is driven through its full range.

Here we can also see that each actuator channel has its own unique offset which can be any value (so long as there is sufficient dynamic range in the digitizer) as it is simply recorded as the target value in the calibration. Note that cross-talk is typically small and it does not prevent the system from closing the loop for diffraction limited correction. It may slow the system down to a minor extent initially (as a few more loop cycles may be required to achieve the zero phase target wavefront error), but since the holographic sensing is orders of magnitude faster than conventional systems, the effect is rarely noticeable.

HALOS uses inexpensive COTS electronics (four XMOS XS1-L8A-64 processors) for sensing and closed-loop control. The system requires a one-off calibration where a plane wave is introduced onto a flattened deformable mirror, to give the desired diffraction-limited, "flat" output. The error function target values for each actuator are then recorded and stored in the microprocessor. Of course, the system could be equally calibrated to any desired output wavefront shape in the same manner. In closed-loop operation, the microprocessor compares the measured error functions at any particular moment to the target values, and from this generates a control signal to drive each actuator to make the appropriate correction. An image of the HALOS set-up is in Fig. 5, along with a magnified image of the hologram lit by white light. The only required equipment not shown in Fig. 5a is the driver and power supply.

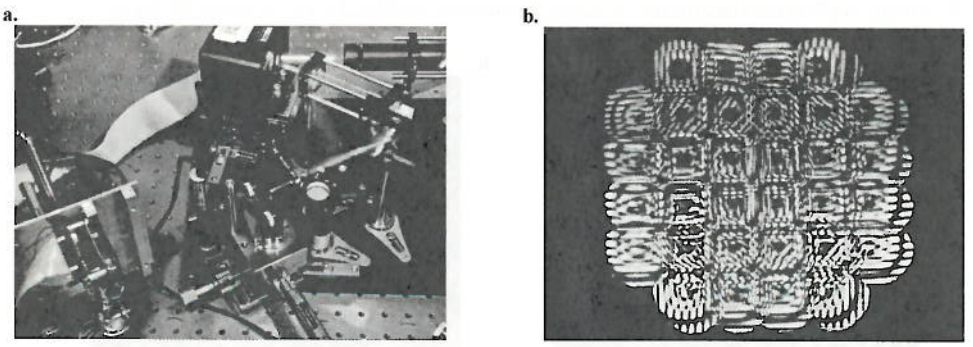

Fig. 5. a. An image of HALOS showing the DM (top center), hologram (right) and sensor (lower left) which was uncovered in this photo to show the electronics. **b.** An image of the hologram showing how the various beams overlap.

The processor power consumption is less than 2.2W and closed-loop latency is 8 microseconds. While this is an order of magnitude better than the best adaptive optics systems, it could be further improved by more than 2 orders of magnitude with more exotic components such as FPGAs or dedicated ASICs. Also, while a computer is used for the initial uploading of the control program and directing the one-off calibration, the closed-loop control is managed entirely by the processor. Thus, no computer is required during closed-loop operation as the system will run autonomously. In our current prototype the computer connection is only used for realtime monitoring of the system performance.

The conventional HALOS configuration (and the one used for experiments described here) uses a beamsplitter to direct part of the beam onto the hologram, while the other portion is the corrected output. However, we can also use a modified design in which the beamsplitter is replaced by a mirror, with all the light directed onto the hologram. In that configuration the undiffracted (zero order) light passing through the hologram can form the output port. This arrangement has the benefit of improving the efficiency at the expense of some dynamic range. The reason is that the hologram may introduce some minor residual aberration to the transmitted beam. In that case, the calibration will require the incorporation of an offset aberration into the deformable mirror to ensure a plane wave output – i.e. instead of the target mirror shape being perfectly flat, it will have some initial distortion.

4. Results

Upstream of the holographic adaptive optics system we added a second MEMS-DM, programmed to introduce a random, time-varying wavefront error. The deformable mirror was located at the same plane as the aperture used for the original recording and this "aberrator" could be used for testing the system performance. Our first test was to measure the true closed-loop bandwidth for the entire system, which involved moving an actuator on the aberrator DM and observing the time taken for the system to sense then full correct for that error. We measured this to be 1ms for the full stroke and faster for correcting minor phase fluctuations. It is important to note that this 1kHz bandwidth is simply a result of inertial limitations in the deformable mirror. The actual electronics themselves have a full loop latency of just 10 microseconds, so with a different deformable mirror the theoretical bandwidth limit is 100kHz.

Next, a time-varying, random aberration was introduced over the entire aperture. The corrected output beam could then be tested to evaluate the correction capability. Fig. 6 shows these results in the form of point spread function and wavefront (interferometric) analyses. Video data is provided as supplemental documentation. Typical values for the wavefront analysis showed that 0.43 waves RMS of aberration could be corrected to 0.16 waves RMS. This could be further improved by increasing the electronics resolution from its current value of 12 bits as well as decreasing the noise in the sensor, feedback circuit and DM driver.

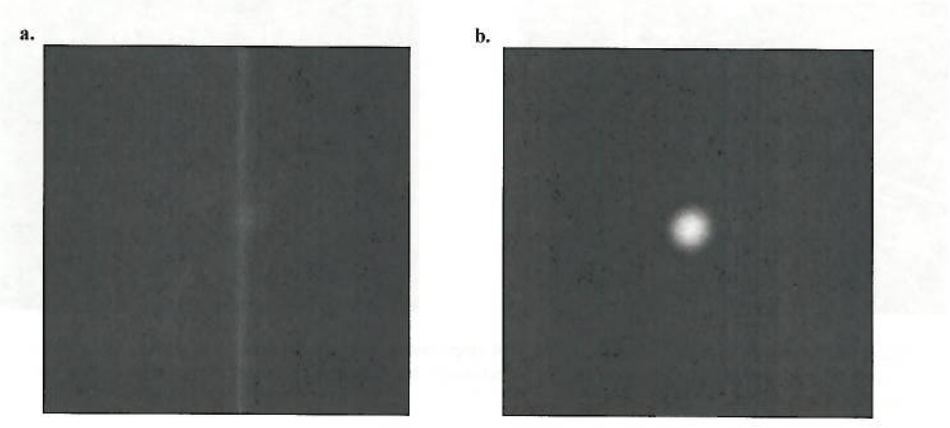

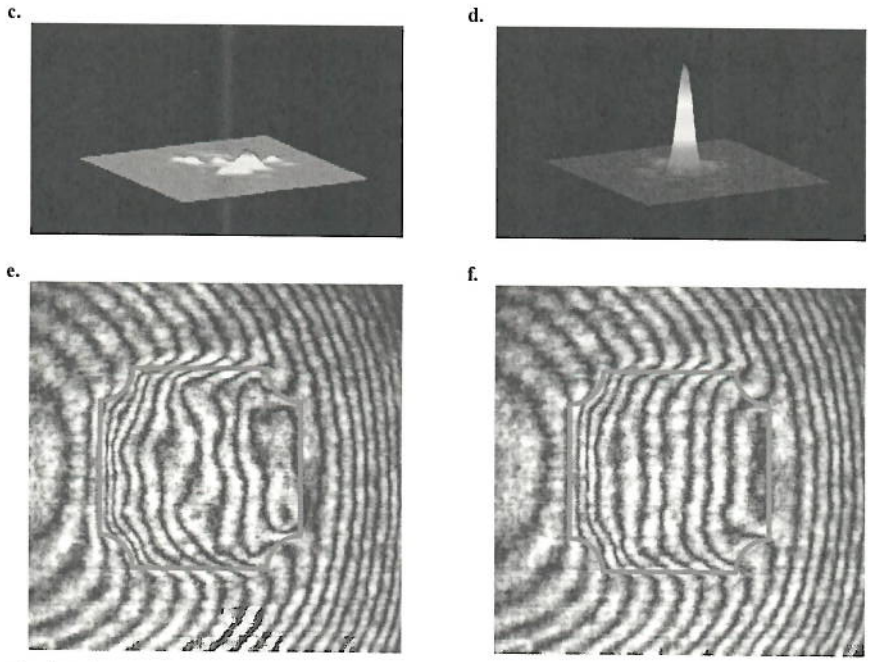

Fig. 6. Point spread function before (**a.**) and after (**b.**) correction. Surface plots generated from these images are shown in (**c.**) and (**d.**), along with a video here. Interferometric analysis of the wavefront before (**c.**) and after (**d.**) correction. The red border indicates the extent of the deformable mirror.

5. Conclusion

We have introduced a holographic adaptive optics system that uses a multiplexed hologram to divide an incoming beam into many focused beams. A measure of the ratio of pairs of spot intensities can be directly related to the absolute position of an actuator in the system's deformable mirror. With a simple circuit, parallel feedback control over individual actuators can be achieved at high speeds. The system has the advantage of being compact, autonomous (computer-free) and scalable to orders more actuators without loss of bandwidth. We have constructed a prototype system consisting of 32 actuators and shown it capable of correcting wavefronts to bandwidths of 1kHz.

Acknowledgements

We wish to acknowledge the support for this project from the United States Air Force Academy the Air Force Office of Scientific Research as well as the High Energy Laser Joint Technology Office.